If the avatar lags, it is not my own: Readiness potential as an objective biomarker of embodiment in virtual reality

Computers in Human Behavior Reports 20 (2025) 100865

Contents lists available at ScienceDirect

Computers in Human Behavior Reports

journal homepage: www.sciencedirect.com/journal/computers-in-human-behavior-reports

Full length article

If the avatar lags, it is not my own: Readiness potential as an objective biomarker of embodiment in virtual reality

Alessandro Piedimonte [a,b,1], Valeria Volpino [a,1], Andrea Bottino [c], Francesco Strada [c,*], Fabio Cielo [c], Francesco Campaci [a,b], Giorgia Cecconato [a], Elisa Carlino [a]

[a] "Rita Levi Montalcini" Department of Neurosciences, University of Turin, Turin 10125, Italy
[b] Carlo Molo Foundation, Turin 10123, Italy
[c] Department of Control and Computer Engineering, Politecnico di Torino, Corso Ducadegli Abruzzi, Turin 10129, Italy

ARTICLE INFO

Keywords:
Agency
Ownership
Virtual reality
EEG
Readiness potential

ABSTRACT

The sense of embodiment — the subjective experience of owning and controlling one's body — is crucial for self-awareness. Virtual Reality (VR) allows controlled manipulation of visuomotor synchrony to investigate embodiment. This study investigates how temporal discrepancies between real and avatar movements affect subjective embodiment and the Readiness Potential (RP), a neurophysiological marker of motor preparation. Using a VR "reach and press" task, participants ($n = 25$) performed movements under three delay conditions (200, 400, 600 ms) and one condition with no added delay (NA-delay), while EEG (64-channel) recorded RP in anterior-frontal and central regions, and subjective embodiment was assessed via questionnaire. A control group performed the NA-delay condition in a real setting. Results showed that embodiment decreased with increasing delay (significant at 400 ms, 600 ms). RP peaks also diminished, particularly frontally, suggesting a shift from motor preparation to cognitive processes like error monitoring. sLORETA implicated dorsal anterior cingulate and prefrontal cortices in monitoring user–avatar discrepancies. These findings highlight RP as an objective biomarker for embodiment in VR. This offers significant implications for human–computer Interaction, providing a continuous, objective measure to improve user agency in VR, enhance neurorehabilitation therapies, optimize avatar design, and advance brain–computer interface systems.

1. Introduction

The sense of body ownership, or the feeling that one's body and its movements belong to the self, is a fundamental aspect of human self-awareness and agency (Braun et al., 2018). This phenomenon has long intrigued researchers across fields such as cognitive neuroscience, psychology, and human–computer interaction (HCI). Recent advances in virtual reality (VR) technologies provide new opportunities for investigating body ownership by allowing individuals to embody virtual avatars and interact with digital environments in increasingly lifelike ways. In this context, the sense of agency (SoA) can be defined as the feeling of being in control of the avatar, and the sense of ownership as the feeling that the virtual avatar is part of one's own body (Argelaguet et al., 2016).

The combination of VR and electroencephalography (EEG) offers a powerful paradigm to investigate the neural underpinnings of embodiment. VR allows for the precise control of visuomotor events, while EEG provides high-temporal-resolution data on the corresponding brain activity. This approach has been used to study *Breaks in Embodiment*, which occur when violations of agency or ownership disrupt the user's experience (Porssut et al., 2019). These studies have shown that event-related potentials (ERPs) elicited by the detection of errors between expected and actual avatar movements can reveal physiological alterations in fronto-central-parietal areas (Porssut et al., 2019; Raz et al., 2020). While crucial, these findings have primarily focused on reactive, error-related brain responses that occur after a discrepancy is detected, leaving proactive markers of the ongoing SoA less explored.

A fundamental way to challenge the SoA is by introducing visuomotor latency, that is, a delay between a user's physical movement and the avatar's corresponding action. Visuomotor delay is known to impair both task performance and the subjective sense of embodiment in VR. Different studies have identified this phenomenon. For example, Waltemate et al. (2016) observed that delays exceeding 125 ms can reduce agency and body ownership, with further deterioration after 300 ms. More recent work suggests that even delays above 100 ms can degrade

* Corresponding author.
E-mail address: francesco.strada@polito.it (F. Strada).
[1] These authors equally contributed.

https://doi.org/10.1016/j.chbr.2025.100865
Received 9 July 2025; Received in revised form 2 October 2025; Accepted 6 November 2025
Available online 12 November 2025

task accuracy and user experience (Caserman et al., 2019). Importantly, user sensitivity to visuomotor delays may vary across populations and tasks. For instance, Samaraweera et al. (2013) demonstrated that mobility-impaired users exhibit gait adjustments in response to delays even without consciously detecting them. Recently, Bockelmann et al. (2024) showed that highly realistic avatars can mitigate some negative effects of delay on embodiment, although the added rendering complexity may itself increase system delays. These studies have provided valuable insights into the behavioral and experiential consequences of visuomotor delays in VR. However, they have not addressed what occurs at the neurophysiological level. In other words, it remains unclear whether objective biomarkers can be identified that reliably track the impact of visuomotor delay on embodiment. Establishing such neural markers would not only complement self-report and behavioral measures but also offer real-time, bias-free indicators of agency and ownership, thus advancing both theoretical understanding and practical applications of VR.

For investigating the neural basis of agency under these conditions, the Readiness Potential (RP) is a more direct and proactive marker than error-related ERPs. As a slow cortical potential that precedes voluntary movement (Kornhuber & Deecke, 1965), the RP reflects motor planning and initiation processes. Its characteristics are tied not only to movement preparation but also to the reliability of action consequences and, notably, the degree of agency and motor control experienced by an individual (Piedimonte et al., 2015; Schurger et al., 2021; Shibasaki & Hallett, 2006; Wen et al., 2018). Despite this theoretical link, EEG correlates of visuomotor discrepancies — such as ERPs or oscillatory power — have been studied (Alchalabi et al., 2019; Esteves et al., 2025; Feder et al., 2023; Kober et al., 2022). However, how varying latency modulates the RP remains largely unexplored.

The present study directly addresses this gap. We investigate how incremental visuomotor delays influence both RP characteristics and the corresponding subjective sense of embodiment during an immersive VR "reach and press" task. We tested four conditions: a no-additional-delay condition (NA-delay, representing baseline system latency), and three conditions with experimentally added delays of 200, 400, and 600 ms. A control group performed the same task in a real-world setting to provide a non-VR comparison. Our results demonstrate that as the delay between real and avatar movements increases, the sense of embodiment significantly decreases. These subjective changes are accompanied by clear electrophysiological alterations: the amplitude of the RP is reduced, particularly in frontal cortical regions, deviating from the classical centrally-dominant pattern.

These findings suggest that the RP can serve as an objective neuromarker for the SoA. This holds significant implications for VR and HCI, offering a continuous, real-time alternative to subjective questionnaires, which are often limited by bias and post-hoc administration (Burns & Fairclough, 2015; Esteves et al., 2025; Guy et al., 2023). Potential applications include enhancing neurorehabilitation through personalized VR therapies (Dewil et al., 2023; Juliano et al., 2020; McDermott et al., 2023), informing avatar and interaction design (Shin et al., 2021; Ziadeh et al., 2021), and advancing Brain–Computer Interface (BCI) technology with more adaptive, 'zero-lag' systems (Brouwer et al., 2017; Kritikos et al., 2023; Nguyen et al., 2024).

2. Materials and methods

2.1. Ethics approval

The present study was conducted in accordance with the Declaration of Helsinki and was approved by the [university name removed for anonymization] ethics committee. All participants provided written informed consent in which the experimental procedure was carefully described.

2.2. Participants

Power analysis was computed with G*Power 3.1 to determine our sample size (Faul et al., 2007; Peck & Gonzalez-Franco, 2021) for electrophysiological variables (peak and time to reach max amplitude) and embodiment questionnaire. To achieve a medium effect size (f = 0.25) with an alpha of 0.05 and power of 0.80, 24 participants were needed. For this reason, 25 individuals took part in this study (mean age = 23.84; SD = 4.65; 16 females, 9 males). Participants were recruited among [university name removed for anonymization] students and were asked to participate in an electrophysiological study aimed at investigating motor performance in VR or real environments. To control for differences between the VR environment (VR group) and real environment (Real group), another 17 participants (mean age = 24.35; SD = 2.39; 10 females, 7 males) were recruited.

2.3. Experimental procedure

As mentioned in the Introduction, this study was designed to investigate the effects of delayed avatar movements on the SoA and RP in a virtual environment. Specifically, the study combined EEG recordings, an immersive virtual experience and hand-tracking technology to investigate how visual-motor discrepancies affect embodiment and motor preparation processes. The participants in the VR group were immersed in a virtual environment that included a chair and a desk with a button, similar to those in the real experimental room, while the rest of the virtual room was furnished with classic elements such as a sofa, a bookshelf, a lamp, and a window (Fig. 1).

Participants sat on the chair in front of the desk and held their right hand over a button. This button was present in both the real and virtual environments so that when participants pressed the button in VR, they also received haptic feedback from the physical button. The position of the button was precisely adjusted in a preliminary calibration phase so that its position in the virtual environment matched that of its real-life counterpart, allowing participants to interact seamlessly with both physical and virtual elements. Each trial began with the hand resting on the button. When a red and white target appeared above the desk at eye level, participants had to release the button and quickly reach the target center with their virtual index finger (Fig. 1). The movement was considered complete when the finger touched the center of the target, after which the target disappeared and the participant returned the hand to the button to prepare for the next trial.

Throughout the experiment, participants saw a virtual representation of their right forearm and hand, which enabled them to orient themselves in space and maintain a coherent body reference. This representation was part of a generic humanoid avatar implemented in Unity and displayed via the Meta Quest 2 headset. Since the headset only provides tracking data for the head and hands, the movement of the virtual arm was generated using inverse kinematics (IK) to ensure a natural and biomechanically plausible animation of the entire limb. The IK was implemented using Unity's built-in Animator IK solver, with the tracked hand position serving as the end effector. This is the standard IK solver included in Unity's humanoid rig and is widely used in VR applications, although the exact algorithmic implementation is not publicly documented. To ensure coherence between the virtual and real-life appearance, the avatar's gender and skin color were matched to each participant (in this study, all were Caucasian). This controlled matching minimized potential confounds associated with avatar–participant mismatch and allowed us to focus specifically on the effects of visuomotor latency on readiness potential.

To track hand movements, we used the Meta Quest 2 built-in optical hand-tracking system. Although such systems can in principle exhibit artifacts (e.g., finger flickering), this was not a problem in our study. Participants performed a simple open-handed reach and press action. Both the start button and the target center (diameter = 5 cm) were equipped with large colliders to ensure reliable interaction detection

Fig. 1. *Left*: The virtual environment experienced during the experiments: Participants were seated on a chair and asked to press the red button on the wooden table. *Right*: Participants' first-person perspective of the VR environment showing the arm and forearm of the controlled avatar as seen through the VR headset. The targets appeared in front of them on top of the table at eye level and had to be touched at the center using the avatar's index finger.

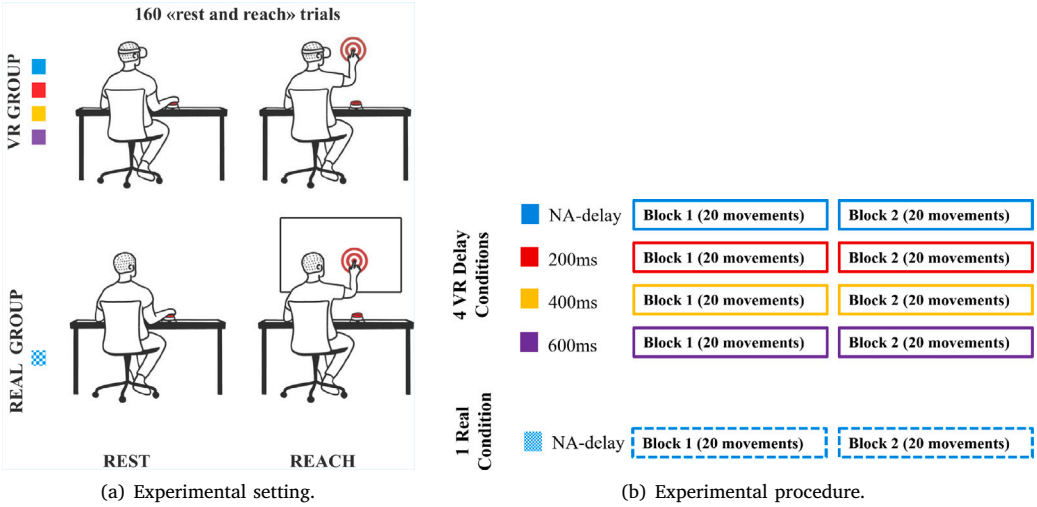

(a) Experimental setting. (b) Experimental procedure.

Fig. 2. In (a) the comparison between the two experimental settings (VR group and Real group). The Real group had no headset and performed the same paradigm, targets appeared in front of them on a specially crafted corkboard, on top of a wooden table at eye level. In (b) an outline of each condition and block of the experimental paradigm.

even in the presence of moderate tracking noise. The room was adequately lit to maximize tracking quality, and no tracking failures were detected in the system logs. Thus, hand-tracking was stable and did not interfere with the embodiment or EEG recordings.

The most important manipulation in this study was the introduction of controlled delays in the movement of the virtual hand. The VR system included a buffer mechanism that temporarily stored the tracking data before they were applied to the virtual hand, effectively delaying the movement of the virtual hand relative to the real hand. This delay was systematically varied across different experimental conditions, allowing the researchers to assess how an increasing temporal shift affected participants' sense of control and neural responses.

The experimental procedure began with the placement and calibration of the EEG cap, which ensured optimal positioning of the electrodes over the motor cortex to capture neural signals related to movement planning. Once the signal quality was confirmed, the VR headset was put on and adjusted to ensure proper alignment and comfort. Once participants were in the virtual environment, they underwent a brief calibration phase aimed at aligning the positions of the virtual table and buttons with their real counterparts to ensure spatial consistency and improve immersion. After calibration, participants had time to adapt to the virtual environment and familiarize themselves with the task and experimental conditions. Once they felt comfortable, the formal experimental session began.

The task consisted of 160 "reach-and-press" movements distributed across the experimental conditions. As stated previously, each movement began with the hand resting on the button and ended when the virtual index finger touched the target center (Fig. 2(a)). After each action, the participants had to put their hand back on the button and press it again to prepare for the next movement. A trigger mounted under the button signaled movement initiation, as already done in other studies (Carlino et al., 2019; Piedimonte et al., 2015). As soon as participants lifted the hand to start the reach, the switch opened and sent a TTL trigger to the EEG system signaling the 0-point, that is the moment when participants started the movement. Each movement was followed by a 7-s rest period before a new target appeared in a different location above the desk. To prevent motor habituation and ensure participants could not anticipate the next movement, the position of the target was pseudo-randomized across five predefined locations throughout the experiment, with the constraint that the same position never occurred consecutively.

The 160 "reach and press" trials were distributed across one matched condition (NA-delay condition) and three mismatched conditions with varying time delays (Fig. 2(b)). In the NA-delay condition, the virtual hand's movements closely resembled participants' real movements with no added delay. Thus, this baseline condition incorporated the inherent latency present in the Meta Quest 2, measured in previous works in the order of 45 ms (Abdlkarim et al., 2024). In contrast, the three mismatched conditions introduced temporal delays of 200, 400, and 600 ms, respectively (i.e., these latencies do not represent total latency but were added to the baseline latency inherent to the system), creating a discrepancy between the participant's actual movements and the ones they observed in VR. For example, in the 400 ms delay condition, the virtual hand left the button 400 ms after the real hand started moving. Participants were not verbally informed about these variations. Each time-delay condition (NA-delay, 200, 400,

600) was repeated twice during the experiment, with each condition involving 40 movements split into two blocks of 20 movements each. Participants completed eight blocks of 20 movements each, presented in a pseudo-randomized order (e.g., NA-delay, 400, 600, 200, 600, NA-delay, 400, 200). The randomization was designed to avoid order effects and ensured that the same condition was never presented twice consecutively. After each block, participants answered four questions adapted from the Embodiment Questionnaire (Peck & Gonzalez-Franco, 2021) to assess their subjective embodiment experience related only to the previous time-delay condition (for details on the questionnaire's administration see the Section 2.4).

The Real group performed the same task in the real environment, outside of VR. As in the VR condition, participants had to keep their hand on the button until the red and white target appeared on a specifically crafted corkboard with circular targets mounted on rotatable supports. Each target had two sides: one identical to the virtual target (white with a red center) and one plain white, matching the background of the panel. During the rest phase, all targets were oriented with the plain white side facing the participant. At the onset of each reaching trial, an experimenter positioned behind the panel manually rotated one target as fast as possible to reveal the red-and-white face, making it visible to the participant and thereby indicating the target location. Once the movement was completed, the target was rotated back to the white side, restoring the rest condition. Five targets were created in five different positions that mimicked the virtual ones. Specifically, five circular targets were mounted on the corkboard at different predefined locations, corresponding to the spatial distribution of targets in the VR environment. This design ensured that participants in the real-world condition experienced comparable spatial variability to those in VR, thereby minimizing potential biases in the comparison between the two settings. Since no artificial lag was introduced in the Real group, the task design was identical to the one in VR, though they only experienced the NA-delay condition.

2.4. Embodiment questionnaire

An adapted version of the Embodiment Questionnaire (Peck & Gonzalez-Franco, 2021) was used to assess participants' sense of embodiment after each block. During the rest period between the blocks, the experimenters asked four questions, which the participants answered on a 7-point Likert scale from "strongly disagree" to "strongly agree". Questions are detailed in Table A.1. The four questions were selected as a subset of the original embodiment questionnaire. Specifically, we chose the items that most directly captured the core dimensions of embodiment relevant to our experimental design: disembodiment (Q1), motor influence (Q2), body ownership (Q3), and agency (Q4). Questions were administered by speaking directly to participants, similarly to other studies focused on the same topic (Tan et al., 2024), and answers were promptly recorded in digital format in an excel spreadsheet. This resulted in eight sets of answers to the four questions (Q1–Q4) across the four conditions (NA-delay,200, 400, 600). The association between each questionnaire and its corresponding delay condition was ensured via the system's log files, in which the condition was recorded together with the start and end time of each block. Finally, the answers belonging to the same condition were averaged, yielding four mean scores (one per condition). These scores are reported in Table A.2 in the Appendix.

2.5. EEG recordings

EEG was recorded at a 1 kHz sampling rate using a 64-channel amplifier and digitizer (Galileo, Ebneuro S. p. A., Italy). Scalp signals were acquired through a prewired cup using 61 shielded Ag-AgCl electrodes, positioned according to the 10-10 International System with CPPz as the reference electrode and FCz as the ground electrode. EEG data processing was carried out using Matlab, via the EEGLAB toolbox (Delorme & Makeig, 2004), and EEG recordings were synchronized to the trigger (i.e., the hand leaving the button to reach the target). The continuous EEG recordings were low-pass filtered using a 30 Hz finite impulse response (FIR) filter. Data was average referenced and then segmented in 2.5 s epochs, ranging between −2000 to +500 ms before and after each trigger. For each participant, a total of 160 epochs was obtained: 40 epochs for each condition (i.e., 0, 200, 400, 600). EOG and muscle artifacts were removed using independent component analysis (ICA) (Jung et al., 2000). In particular, ICs related to eye movements and muscle noise were removed using an EEGLAB plugin, namely ICLabel (Pion-Tonachini et al., 2019), set to automatically remove components recognized as eye movements and muscle activity with a 90% confidence threshold. Baseline correction was performed by subtracting the −2000 to −1500 ms pre-stimulus interval. Finally, epochs exceeding ±75 μV were automatically removed. Artifact-free epochs were averaged for each condition and each participant and handled accordingly, thus, for each participant, we obtained four averages.

Given the heterogeneity of self-regulating processes in the frontocentral networks (Menon & D'Esposito, 2022) and the specificity of motor processes over the motor cortical areas (Kim et al., 2023; Suviseshamuthu et al., 2022), RPs averages have been computed on two distinct fronto-central patches. Analyzed electrodes were grouped as follows: AF3, AFz, F1, F3, F5, Fz for the Anterior-Frontal patch (AF), and C1, C3, C5, Cz for the Central patch (C).

A subsequent ERPs computation was carried out using sLORETA software (Pascual-Marqui, 2002) to estimate the current source density values. sLORETA computes a three-dimensional distributed source localization to solve the inverse problem of brain electric activity to calculate the standardized current source density (amperes per square meter; A/m^2) at each of the 6.239 gray matter and hippocampus voxels of the probabilistic MNI-reference brain template (resolution: 5 mm × 5 mm × 5 mm) by the Brain Imaging Center of the Montreal Neurological Institute (Mazziotta et al., 2001). The calculation of the current source density is derived from a linearly weighted sum of scalp electric potentials. sLORETA estimates the underlying sources based on the assumption that neighboring voxels exhibit maximally similar electrical activity. sLORETA assumes a smooth spatial distribution of electrical activity, applying the principle that neighboring voxels should exhibit highly similar activity (Silva et al., 1991). This approach reduces localization errors and enables the accurate identification of source activity, albeit with low spatial resolution.

2.6. Statistical analysis

Statistical analyses on the behavioral and ERPs data were carried out using Statistica Software (StatSoft, 2011). Analyses on source localization were carried out using the statistical package of sLORETA (Pascual-Marqui, 2002). The Kolmogorov–Smirnov test was used to verify the normality of the distribution of all the dependent variables. For the behavioral and ERPs analyses, the level of significance was set at $p < 0.05$, data in the figures are presented as mean±standard error of the mean (SEM). For sLORETA analyses the level of significance was set at $p < 0.01$.

2.7. Embodiment questionnaire analysis

To analyze the sense of embodiment in the VR group, two complementary analyses were performed. First, mean Likert scores (1–7) across all questionnaire items (Q1–Q4) were entered into a repeated-measures ANOVA with Condition (NA-delay, 200, 400, 600 ms) as the within-subject factor. Second, each item was analyzed separately to examine whether the observed effects were consistent across individual questions. For both analyses, post hoc Student–Newman–Keuls (SNK) tests were applied to explore pairwise differences between conditions. Moreover, a correlation analysis was conducted to examine the relationship between electrophysiological indices of motor preparation and subjective embodiment ratings.

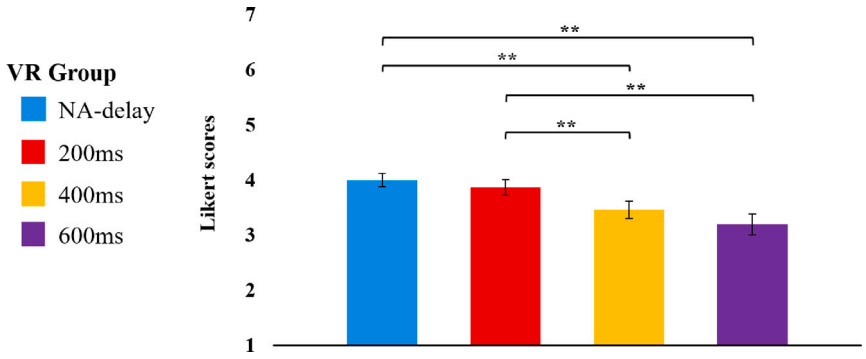

Fig. 3. Embodiment questionnaire results of average items. The *Y*-axis represents the Likert 1–7 scores. Each colored bar corresponds to a different delay condition. Asterisks denote statistically significant post hoc differences: $^{**}p < 0.01$. Error bars represent standard errors of the means (SEM).

2.8. Readiness potential analysis

Differences in mean RP peak and time at max amplitude for every electrode patch in the VR group were tested by means of a two repeated-measures ANOVAs with Condition (0, 200, 400, 600) as the within-subject factor. To investigate significant differences, post hoc SNK test was applied for multiple comparisons. Mauchly's test was performed to detect sphericity violations. In cases where sphericity assumption was violated, Greenhouse–Geisser (G–G) corrected degrees of freedom were applied to adjust the p-values and results were reported using G–G correction. Given the unbalanced group sizes (Real = 17; VR = 25), we performed Levene's test for homogeneity of variances on the EEG patches (Anterior-Frontal, Central). Results indicated that variances were not homogeneous between groups (AF: $p = 0.030$; C: $p = 0.013$). Based on this violation of the homogeneity assumption, a non-parametric test (Mann–Whitney U test) was performed, which do not rely on distributional or variance homogeneity assumptions, on both RP peak and time at max amplitude to check for differences between groups in the NA-delay.

2.9. EEG source analysis

Current source densities in each voxel as results of the differences between two conditions or groups (e.g., VR group > Real group) were computed using statistical non-parametric mapping by sLORETA software (Nichols & Holmes, 2002). This method averages intracerebral current densities distribution at a specific time interval and returns as output significant differences based on a voxel-by-voxel one-tailed paired or independent samples t-test with 5.000 permutations. Activated voxels exceeding the tcrit are considered as cortical active regions and classified through Broadmann areas (Zilles & Amunts, 2010) and normalized MNI coordinates (Mazziotta et al., 2001).

3. Results

3.1. Embodiment questionnaire

Behavioral results of the mean Likert scores (1–7) across all questionnaire items (Q1–Q4) are shown in Fig. 3. Means of single items are reported in Table A.2. For the overall sense of embodiment, the analysis on mean Likert score points (1–7) for questions Q1, Q2, Q3, and Q4 showed a significant main effect of Condition ($F_{(3,72)} = 12.85$, $p < 0.01$), depicting a decrease in mean scores from the NA-delay condition to the 600 ms delay condition. SNK post hoc test showed significant differences between the NA-delay condition and the 400 ms ($p < 0.01$) and 600 ms ($p < 0.01$) delay conditions, and between the 200 ms condition and both the 400 ms ($p < 0,01$) and 600 ms ($p < 0.01$) delay conditions, but not between the 0 ms and the 200 ms ($p = 0.371$) delay condition, and between the 400 ms and the 600 ms ($p = 0,094$) delay conditions.

Furthermore, we analyzed each item separately to examine whether the observed effects were consistent across individual questions.

Results for Q1 showed that the repeated-measures ANOVA on mean Likert ratings did not reveal a significant main effect of Condition, $F_{(3,72)} = 0.48$, $p = 0.698$.

Results for Q2 showed a significant main effect of Condition, $F_{(3,72)} = 7.67$, $p < 0.001$. Since Mauchly's test indicated that the assumption of sphericity was violated, the Greenhouse–Geisser correction was applied ($\varepsilon = 0.667$). After applying the Greenhouse–Geisser correction, the effect of Condition remained significant, $F_{(2.00,48.02)} = 7.67$, $p < 0.001$. Post-hoc SNK comparisons revealed that the NA-delay condition significantly differed from both the 400 ms ($p < 0.05$) and 600 ms ($p < 0.001$) conditions, and the 200 ms condition significantly differed from the 600 ms condition ($p = 0.01$). No significant differences were found between NA-delay and 200 ms ($p = 0.366$), between 200 ms and 400 ms ($p = 0.093$), and between 400 ms and 600 ms ($p = 0.072$).

Results for Q3 showed a significant main effect of Condition, $F_{(3,72)} = 36.16$, $p < 0.001$. Since Mauchly's test indicated a violation of sphericity, the Greenhouse–Geisser correction was applied ($\varepsilon = 0.738$). The effect of Condition remained highly significant after correction, $F_{(2.22,53.17)} = 36.16$, $p < 0.001$. Post-hoc SNK tests revealed significant differences between the NA-delay condition and both the 400 ms ($p < 0.001$) and 600 ms ($p < 0.001$) conditions, but not between NA-delay and 200 ms ($p = 0.072$). Furthermore, the 200 ms condition significantly differed from the 400 ms ($p < 0.001$) and 600 ms ($p < 0.001$) conditions, while the 400 ms and 600 ms conditions also differed significantly ($p < 0.001$).

Results for Q4 showed a significant main effect of Condition, $F_{(3,72)} = 34.87$, $p < 0.001$. Since Mauchly's test indicated a violation of sphericity, the Greenhouse–Geisser correction was applied ($\varepsilon = 0.594$). The effect of Condition remained highly significant after correction, $F_{(1.78,42.75)} = 34.87$, $p < 0.001$. Post-hoc SNK tests revealed that the NA-delay condition significantly differed from the 400 ms ($p < 0.001$) and 600 ms ($p < 0.001$) conditions, but not from the 200 ms condition ($p = 0.227$). In addition, the 200 ms condition significantly differed from both the 400 ms ($p < 0.001$) and 600 ms ($p < 0.001$) conditions, while the 400 ms and 600 ms conditions also significantly differed ($p < 0.01$). To summarize, results showed that all items, with the exception of Q1, yielded patterns comparable to the overall analysis, confirming the robustness of the effect across individual questions.

3.2. Readiness potential peak and time at max amplitude in the VR group

Electrophysiological results for the VR group are shown in Fig. 4. For the Anterior-Frontal patch, the analysis on the mean RPs peak showed a significant main effect of Condition ($F_{(3,72)} = 3.46$, $p < 0.05$), revealing a decrease in mean RPs peak from the NA-delay condition to the other conditions with longer delays. Mauchly's test indicated that the assumption of sphericity had been violated ($W = 0.486$, $\chi^2(5) = 16.40$, $p < 0.01$). Therefore, degrees of freedom were corrected using the Greenhouse–Geisser estimate of sphericity ($\varepsilon = 0.671$). The effect of condition remained significant after correction, $F_{(2.01,48.33)} = 3.46$,

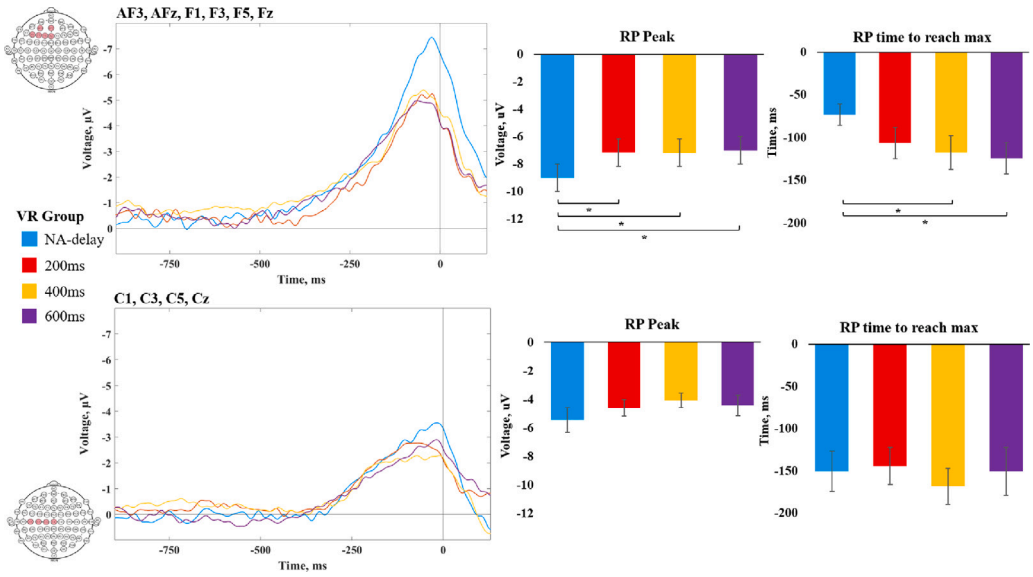

Fig. 4. EEG results for RPs in the VR group. *Left*: Grand-average RP waveforms (in μV) for each delay condition across all participants. The top plot shows the Anterior-Frontal patch (AF3, AFz, F1, F3, F5, Fz), while the bottom plot shows the Central patch (C1, C3, C5, Cz). The 0 point on the x-axis represents the movement initiation (e.g., the time when the hand leaves the button). *Center*: Bar plots showing the mean (±SEM) of individual participants' RP peak amplitudes. Note that these values differ from the grand-average waveforms due to inter-participant timing variability. *Right*: Bar plots showing RP latency, defined as the time of maximum amplitude. Asterisks denote statistically significant post hoc differences: $^{*}p < 0.05$, $^{**}p < 0.01$. Error bars represent standard error of the mean (SEM).

$p < 0.05$. SNK post hoc test showed significant differences between the NA-delay condition and the 200 ms ($p < 0.05$), 400 ms ($p < 0.05$), and 600 ms ($p < 0.05$) delay conditions. No significant differences were found between the 200 ms, the 400 ms, and the 600 ms delay conditions. For the Central patch, the analysis on the mean RPs peak showed no significant effect of Condition ($F_{(3,72)} = 2.08$, $p = 0.111$), nor significant SNK post hoc test differences.

For the Anterior-Frontal patch, the analysis of the mean RPs latency showed a significant main effect of Condition ($F_{(3,72)} = 3.51$, $p < 0.05$), revealing an increased mean RP time to reach max amplitude in the NA-delay condition compared to the other conditions with longer delays. Mauchly's test indicated that the assumption of sphericity had been violated, and thus Greenhouse–Geisser corrected degrees of freedom were applied ($\varepsilon = 0.750$). The effect of condition remained significant after correction ($F_{(2.25,53.97)} = 3.52$, $p < 0.05$). SNK post hoc test showed significant differences between the NA-delay condition and the 400 ms ($p < 0.05$) and 600 ms ($p < 0.05$) delay conditions, while only a tendency towards significance was found between the NA-delay condition and the 200 ms delay condition ($p = 0.056$). No significant differences were found between the 200 ms, the 400 ms, and the 600 ms delay conditions. For the Central patch, the analysis on the mean RPs latency showed no significant effect of Condition ($F_{(3,72)} = 0.29$, $p = 0.834$), nor significant SNK post hoc test differences.

3.3. Readiness potential peak in the VR vs. Real group

Electrophysiological results for the VR group vs. Real group are shown in Fig. 5. For the Anterior-Frontal patch, the analysis on mean RPs peak (NA-delay condition) showed a significant difference between groups ($U = 82.0$, $Z = 3.34$, $p < 0.01$), revealing a higher RP peak in the VR group compared to the Real group. For the Central patch, the analysis on the mean RPs peak (NA-delay condition) showed no significant effect of Group ($U = 169.0$, $Z = 1.11$, $p = 0.265$), revealing no difference between the VR group and the Real group.

3.4. Readiness potential time at max amplitude in the VR vs. real group

For the Anterior-Frontal patch, the analysis of mean RPs time to max amplitude (NA-delay condition) showed a significant difference between groups ($U = 131.0$, $Z = -2.09$, $p < 0.05$), revealing a delayed RP time at max amplitude in the VR group compared to the Real group. For the Central patch, the analysis on the mean RPs time at max amplitude (NA-delay condition) showed a significant difference between groups ($U = 133.5$, $Z = 2.02$, $p < 0.05$), revealing an earlier RP time at max amplitude in the VR group compared to the Real group, as opposed to the Anterior-Frontal patch.

3.5. sLORETA source localization in the VR group

The comparison between experimental conditions NA-delay > 200-delay in the averaged time window −200 ms – 0 ms (corresponding to the Readiness Potential peak) showed statistically significant greater cortical activations in the bilateral anterior cingulate cortex (BAs 24, 32, 33), the bilateral medial frontal gyrus (BA 9), the bilateral cingulate gyrus (BAs 24, 32), the right insula (BA 13), the right postcentral gyrus (BAs 2,3), the right superior frontal gyrus (BAs 9,10), the right inferior parietal lobule (BA 40), the middle frontal gyrus (BA 10), and in the right precentral gyrus (BA 4). See Fig. 6 for the activation map and Table B.3 for anatomical details.

The comparison between experimental conditions NA-delay > 400-delay in the averaged time window −200 ms – 0 ms showed statistically significant higher cortical activations in the bilateral cingulate gyrus (BAs 6, 23, 24, 32), the bilateral anterior cingulate cortex (BAs 24, 32, 33), the bilateral medial frontal gyrus (BAs 6, 9), the left insula (BA 13), the right superior frontal gyrus (BA 9), the right postcentral gyrus (BAs 2,3), the right precentral gyrus (BAs 4,6), and in the right inferior parietal lobule (BA 40). See Fig. 7 for the activation map and Table B.4 for anatomical details.

The comparison between experimental conditions NA-delay > 600-delay in the averaged time window -200 ms – 0 ms showed statistically significant higher cortical activations in the bilateral frontal gyrus (BAs, 6, 8, 9), the bilateral cingulate gyrus (BAs 6, 24, 32), the bilateral anterior cingulate (BAs 24, 32, 33), the bilateral superior frontal gyrus (BAs 6, 8), the left precentral gyrus (BA 6), and in the left middle frontal gyrus (BA 6). See Fig. 8 for the activation map and Table B.5 for anatomical details.

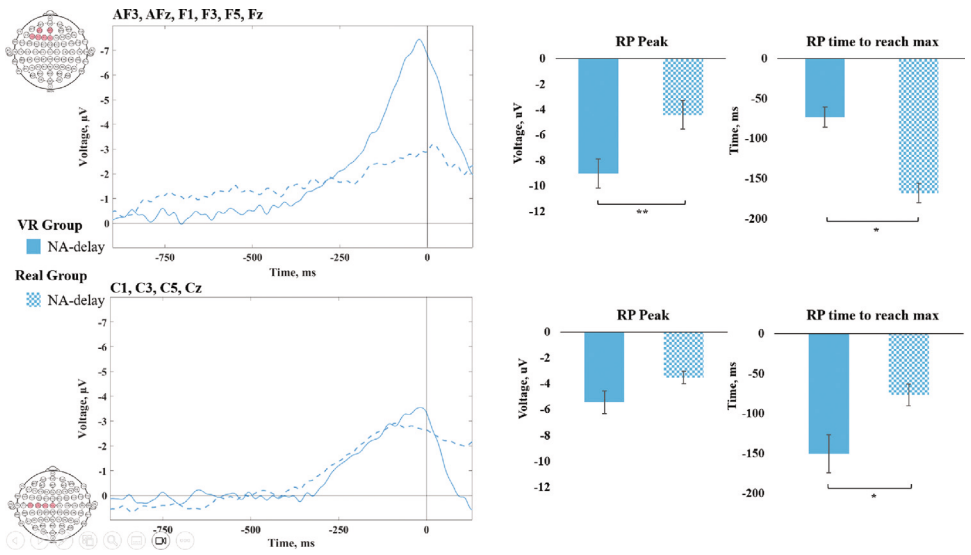

Fig. 5. EEG results for RPs comparing the VR group and the Real group. *Left*: Grand-average RP waveforms (in μV) for the NA-delay condition. Solid blue lines represent the VR group, and dashed blue lines represent the Real group. The top plot shows the Anterior-Frontal patch (AF3, AFz, F1, F3, F5, Fz), while the bottom plot shows the Central patch (C1, C3, C5, Cz). The 0 point on the x-axis represents the movement initiation (e.g., the time when the hand leaves the button). *Center*: Bar plots showing the mean (±SEM) of individual participants' RP peak amplitudes. Note that these values differ from the grand-average waveforms due to inter-participant timing variability. *Right*: Bar plots showing RP latency, defined as the time of maximum amplitude. Asterisks indicate statistically significant differences between groups: $p < 0.05$, $^*p < 0.01$. Error bars represent standard error of the mean (SEM).

3.6. sLORETA source localization in the VR vs. Real group

The comparison between experimental groups VR group > Real group in the averaged time window −200 ms – 0 ms showed statistically significant higher cortical activations (corresponding to the Readiness Potential peak) showed statistically significant higher cortical activations in the left superior frontal gyrus (BAs 9,10), the left middle frontal gyrus (BAs 9,10), and in the left medial frontal gyrus (BA 10). See Fig. 9 for the activation map and Table B.6 for anatomical details.

3.7. Correlation analysis between RP peak and time at max amplitude and subjective embodiment

An exploratory correlation analysis was conducted to examine the relationship between electrophysiological indices of motor preparation and subjective embodiment ratings. A mixed-model approach was used to account for within-subject variability across conditions (NA-delay, 200, 400, 600 ms). In these models, questionnaire responses were entered as dependent variables, and separate analyses were run for Q3 ("I felt as if the virtual body was my body") and Q4 ("I felt like I could control the virtual body as if it was my own body"). RP peak and RP time at maximum amplitude in Anterior-Frontal patch (the only significant patch) were included as fixed covariates of interest, while Condition (NA-delay, 200, 400, 600 ms) was modeled as a fixed factor. Subject was specified as a random factor to account for repeated measures across participants. Degrees of freedom for fixed effects were estimated using the Satterthwaite approximation, which provides more accurate p-values in mixed models with unbalanced designs. This approach allowed us to test whether within-participant variation in RP variables was systematically related to embodiment ratings, while simultaneously controlling for Condition effects and between-subject differences.

No significant differences were observed for RP peak amplitude either for Q3 or for Q4. In contrast, considering RP time at max amplitude, for Q3 the model revealed a significant effect of RP time at maximum amplitude ($F_{1,30.95} = 6.14$, $p < 0.05$), and a significant effect of Condition ($F_{3,77.45} = 30.83$, $p < 0.001$). The random effect of Subject was also significant ($F_{24,71} = 4.32$, $p < 0.001$). For Q4, results similarly showed a significant effect of RP time at max amplitude ($F_{1,35.73} = 7.19$, $p < 0.05$), alongside a robust main effect of Condition ($F_{3,74.98} = 30.28$, $p < 0.001$), and a significant random effect of Subject ($F_{24,71} = 2.61$, $p < 0.001$). These results suggest that RP time to reach max amplitude is a robust predictor of subjective embodiment.

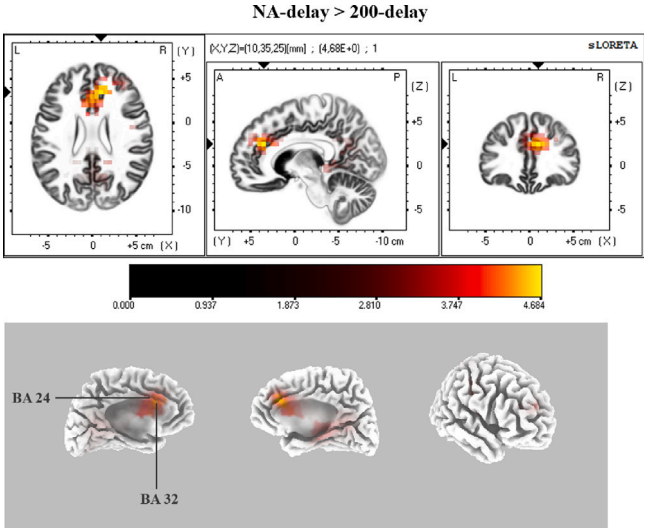

Fig. 6. sLORETA source localization results for the contrast NA-delay > 200-delay. Activated voxels (thresholded at $p < 0.01$, corrected for multiple comparisons) are shown in yellow and red. Peak cortical activity was found in the anterior cingulate cortex, specifically in BA 32. Maps were generated using statistical non-parametric mapping (SnPM), co-registered to Talairach space based on the MNI-152 template and the Co-Planar Stereotaxic Atlas of the human brain.

4. Discussion

In the current study, using an immersive VR environment, we investigated how increasing latency between a participant's real movement and their avatar's movement affects both the subjective sense of ownership and the neurophysiological markers of motor preparation, specifically the RP's peak amplitude and time to reach max amplitude. Interestingly, our findings indicate that as the delay between the real and

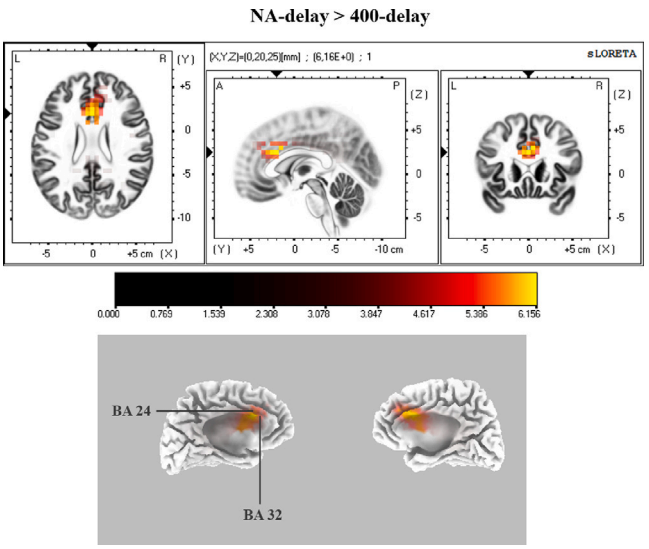

Fig. 7. sLORETA results for the contrast NA-delay > 400-delay. See Fig. 6 for methods. Peak activation was again localized to the anterior cingulate cortex (BA 32).

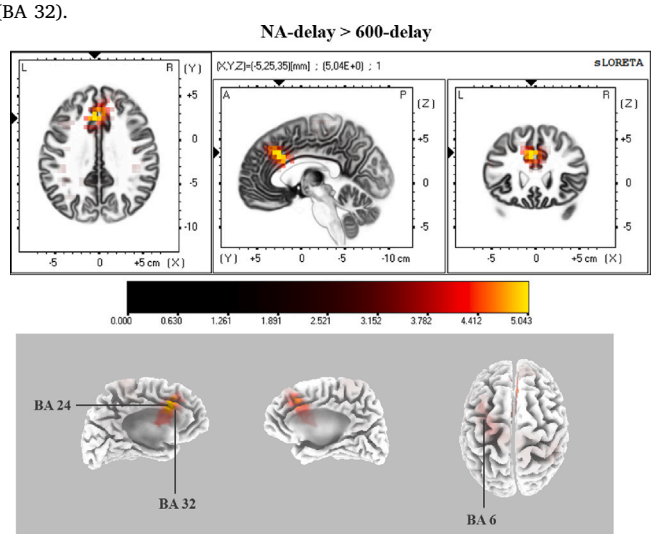

Fig. 8. sLORETA results for the contrast NA-delay > 600-delay. See Fig. 6 for methods. Peak activation was observed in the cingulate cortex (BA 32).

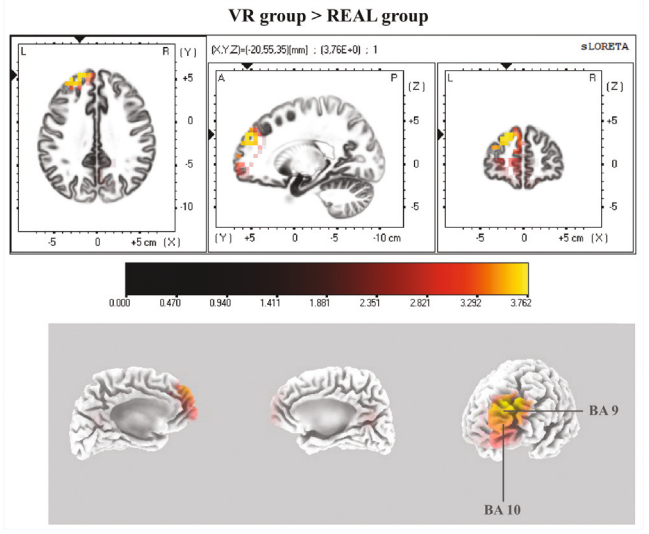

Fig. 9. sLORETA results for the contrast VR > Real group. See Fig. 6 for methods. Peak activation was located in the superior frontal gyrus (BA 9).

avatar's movement changes from the NA-delay condition to the other conditions with added delays (i.e. 200, 400, 600), the amplitude of the RP as well as the time at maximum amplitude both decrease, particularly in frontal regions, representing a departure from the classic pattern of central RP peaks. Accompanying these electrophysiological differences, participants' sense of embodiment, particularly measured in questions 3 and 4 specifically related to agency, significantly decreases in the 400 ms and 600 ms added delay condition compared to the NA-delay condition. Furthermore, a direct comparison of the NA-delay condition revealed that the VR group exhibited a higher and temporally delayed RP peak in frontal cortical regions relative to the Real group.

Albeit from a behavioral point of view, a similar situation where time has been shown to be crucial to determine the sense of embodiment is depicted by studies investigating the rubber hand illusion (RHI), which involves attributing sensations from a real hand to a rubber hand when both are simultaneously stimulated (Botvinick & Cohen, 1998). Using this specific paradigm, it was possible to show that temporal visuotactile synchronization is needed to create the sense of ownership of the visible stroked fake hand, since when the visual delay increased compared to the tactile stimulation, the illusion strength significantly decreased (Shibuya et al., 2019) giving rise to a similar loss of the sense of embodiment recorded in our longest delay conditions. Indeed, delay in time between volition and action execution seems to be crucial to creating a strong link bond between what is moving, e.g. an arm, and its ownership, e.g. my arm, as synchronization between one own's intention to move and a specific movement is one of the main characteristics of conscious will (Wegner & Wheatley, 1999). Interestingly, from an electrophysiological perspective, it has been shown that reducing perceptions of being in control of one's own actions via verbally undermining beliefs in free will result in a reduction of the amplitude of RP (Rigoni et al., 2011).

Taking these studies into account, it is possible to explain the reduction of the RP amplitude observed in the frontal electrodes during the delayed conditions as a reduction in being in control of one own's actions when the only action observable by participants, that is the avatar movement, completely diverged from their own movement, i.e. it was out of participants' control. This reduction was also underlined by the significantly lower scores in the sense of embodiment scales, recorded after the longest delay conditions. On the other hand, the significantly higher RP amplitude in the NA-delay condition could represent an increased activation of the premotor areas involved in RP generation to exert control over the avatar arm while programming the reaching movement in the VR environment while the illusion of embodiment was still not broken.

This last hypothesis is also in line with data regarding the time for RP to reach max amplitude in the different delay conditions, as in the NA-delay condition RP showed a significantly longer time to reach max amplitude in comparison to the other conditions, in particular with 400 ms and 600 ms delays.

Rather than showing a gradual decrease in peak latency, our study revealed a significant step change with the addition of all longer latencies, mirroring the pattern observed for amplitude. When considering the Meta Quest 2's inherent latency of approximately 45–50 ms (Abdlkarim et al., 2024), the significant decrease beginning at the 200 ms added delay condition corresponds to a total system latency approaching 250 ms. This threshold is particularly noteworthy, as classic literature has established that agency diminishes when delays between actions and outcomes exceed approximately 250 ms. This timing aligns with research on temporal binding — the subjective compression of intervals between causally related events — which serves as an implicit measure of agency (also known as intentional binding). Studies have demonstrated that this binding effect diminishes when action-outcome intervals reach or exceed 250 ms (Ruess et al., 2017). More recent electrophysiological work in brain–computer interfaces has further confirmed this threshold, showing that reports of agency are more likely when actions occur within 250 ms of a Readiness Potential compared to

when no RP is present in the preceding 250 ms (Schultze-Kraft et al., 2020). Our findings clearly align with this established literature. The linear mixed model results, which link decreased agency scores (embodiment questionnaire items Q3 and Q4) to reduced time at maximum amplitude starting from the 200 ms condition, suggest that this RP measure effectively captures the disruption of the sensorimotor connection between participants and their avatars. Thus, time at maximum amplitude appears to serve as a reliable neural marker for the breakdown of embodiment when visuomotor delays exceed perceptual thresholds.

Again, this slower RP timing in the NA-delay and partially in the 200 ms condition could account for a longer elaboration of the possible discrepancies between the actual and the virtual movement (i.e. they were absent or small enough to be difficult to detect) while during longer delays with actual and virtual movements overtly decoupled, elaboration time was significantly reduced. Indeed, this is in line with a recent EEG study where participants were asked to either select a specific action among different actions or execute, without selecting it, the same action and results clearly showed longer RP's timing in the selection task, possibly due to what the authors called "evidence accumulation process for response selection in the motor system" (Lui et al., 2021). Interestingly, all these RP-related differences were observed mainly in frontal electrodes rather than the more typical central ones (i.e., those related to primary motor areas). This highlights a possible shift from a simple action programming to higher functions such as error detection, goal directed behaviors and decision making.

In agreement with this last observation, activation distribution related to RP's peaks investigated with sLORETA showed a predominant activation of frontal areas in the NA-delay condition in comparison to the other conditions, with the involvement of premotor areas such as Brodmann area 6 when compared with the longest, 600 ms, delay where participants' sense of embodiment significantly decreased. One possible explanation for the hyperactivation of these areas during the no-delay VR condition is that these cortical regions could be trying to maintain a strong sense of embodiment between the real arm and the avatar arm while the significantly less activation in these areas, in particular during the 600 ms latency, could represent the disruption of such link. This hypothesis is supported by classic studies on the sense of embodiment. For instance, studies conducted with patients affected by pathological embodiment, the delusion that someone else's arm belongs to one's own body, showed that when someone else's arm is positioned like the patient's own, the patient perceives it as part of their body and if this newly acquired 'alien' arm moves, the patient believes their own arm has moved, becoming unaware of the difference while the arm is present (Garbarini et al., 2014, 2013). Interestingly, the lesions characterizing these patients involved subcortical areas such as the superior longitudinal fasciculus while systematically spared specific frontal areas such as the premotor cortex (Brodmann area 6), identified by the authors as the primary region responsible of maintaining a strong sense of embodiment in these patients when incorporating alien arms (Pia et al., 2020). Similar observations, albeit on healthy participants, have been made using the abovementioned rubber-hand illusion highlighting how the feeling of ownership towards the fake hand seems to be related to stronger activations in premotor areas (Ehrsson et al., 2004; Grivaz et al., 2017). Thus, based on this literature and our data, it is possible that premotor areas exerted maximum activity, in the NA-delay condition, to incorporate the alien, i.e. avatar, hand into participants own body representation until the temporal gap between the real and virtual condition became too wide and the "avatar illusion" was dissolved.

Notably, the sLORETA analysis showed also the significant involvement of other medial areas such as parts of the dorsal anterior cingulate cortex (dACC), namely Brodmann areas 24 and 32. In particular, it was again observed a higher activation of these areas in the NA-delay condition in comparison to the other conditions. These areas have been classically described as the center of performance monitoring via error detection (Carter et al. 1998) and then incorporated into a complex network related to goal-directed behaviors (Apps, 2018). More recently, activations of these regions were also observed in a study where participants were asked to decide whether a stretched and rotated arm was a right or a left arm and the authors concluded that dACC could be important in "integrating intero-exteroceptive cues for the purpose of spatially transforming the image of our self-body" (Sasaoka et al., 2024). Thus, the higher activation of the dACC in the NA-delay condition could entail a higher burden in detecting the discrepancies between the real and the avatar movement while the lower activation observed in the longer delay conditions could describe the lack of this necessity since the two movements have been already detected as separated, mirroring the observed subjective decrease in the sense of embodiment.

Finally, the comparison between VR and Real groups (NA-delay condition) showed in the frontal electrodes a higher amplitude of the RPs as well as a longer time to reach max amplitude in participants performing the reaching movement in the VR environment. Similarly to what has been discussed before, this result highlights the possibility for RP to represent movement preparation while trying to incorporate the avatar's action when its characteristics almost perfectly overlap those produced in the real environment. Following this line of thought, the real environment is more akin to the VR condition with a 600 ms delay since, with this delay, the avatar and the real participant represented two different agents and within this VR condition a reaching movement was programmed without taking into account the avatar arm exactly as if it was executed in a real environment. In other words, while with no VR there is no embodiment, in a VR condition with excessive latency, the embodiment of the avatar is disrupted.

Notably, sLORETA showed a significantly higher activation in the VR group compared to the Real group in a specific group of frontal areas located in the left frontal gyrus, namely Brodmann area 9 and 10. Activity within these areas has been principally related to motor imagery, i.e. the ability to imagine movements without executing them, and is also in line with the current neuroimaging literature related to VR environments. For instance, it has been observed that activation in the dorsolateral prefrontal cortex (DLPFC), an area roughly corresponding to Brodmann area 9, is associated in VR with the experience of presence (Jäncke et al., 2009), an early definition of the subjective feeling of being in a virtual environment while being unaware of the real surroundings (Meehan et al., 2002). Furthermore, while motor imagery and execution share a similar neural network, it has been observed how imagining movements with one hand elicits activation of specific cortical and subcortical areas, with prefrontal areas such as Broadmann area 10 among them Gerardin et al. (2000) and more in general motor imagery regarding finger movements have been related to activity in the middle frontal gyrus (Hanakawa et al., 2003). Thus, it is possible that movements executed in a virtual space share some similarities with imagined movements, an idea that has been already engaged with in motor training as well as rehabilitation protocols where it has been proved that motor imagery accompanied with VR environments is capable of increasing cortical excitability in stroke patients and healthy participants more than motor imagery alone (Im et al., 2016) as well as improving shot accuracy in curling, bowling, and archery (Bedir & Erhan, 2021). It is also interesting to note that left frontal gyrus lesions can lead to ideomotor apraxia, which is a neuropsychological pathology where goal-directed actions are severely impaired (Haaland et al., 2000) highlighting the importance of these left frontal regions to control complex movements with a specific goal, which in our experiment could be well represented by reaching a random target in a virtual environment.

Overall, our data suggests that in VR environments where agency and ownership are challenged by temporal discrepancies, the brain's motor preparation processes may shift from the motor areas to more frontal regions implicated in higher-order cognitive functions such as error monitoring, agency evaluation, and decision-making (Kornhuber & Deecke, 1965).

Building upon these neurophysiological insights, the finding that the RP is sensitive to visuomotor delay in immersive VR has potentially valuable implications for HCI and VR research. This observation

suggests a possible pathway towards objectively monitoring aspects of a user's SoA—a subjective psychological construct that has traditionally relied on post-hoc, self-report measures. Traditionally, assessing user experience relies on subjective questionnaires, which are often criticized for their inherent limitations. These methods are prone to participant interpretation and scale biases, lack real-time insight, and necessitate interrupting the immersive flow, preventing them from being considered a "gold standard" for SoA assessment (Burns & Fairclough, 2015; Esteves et al., 2025; Guy et al., 2023; Safikhani et al., 2024). By leveraging the high temporal resolution and increasing portability of EEG (Nguyen et al., 2024; Nwagu et al., 2023), these findings provide a continuous, objective, and non-intrusive method to quantify SoA, offering more reliable insights into how users genuinely perceive their control and engagement within virtual worlds. This directly addresses a critical need for definitive EEG biomarkers for agency, bridging the gap between self-reported experiences and objective neurophysiological evidence (Esteves et al., 2025; Jeunet et al., 2018).

These findings may also have a significant impact on the enhancement of neurorehabilitation and therapeutic VR applications (Dewil et al., 2023). In VR-based rehabilitation, particularly for gait and motor function recovery, a continuous and objective measure of embodiment and agency is paramount for maximizing therapeutic efficacy (Alchalabi et al., 2019; Dewil et al., 2023). A heightened SoA is directly associated with improved perceived movement control and better functional performance (Dewil et al., 2023). Real-time SoA measurement would allow therapists and rehabilitation systems to monitor and maintain optimal levels of agency and engagement throughout training sessions, which is crucial for fostering neuroplasticity and recovery (Dewil et al., 2023; Vourvopoulos et al., 2024). Importantly, this approach can help prevent feelings of estrangement or distress that may arise when patients feel a lack of control, potentially hindering recovery in BCI-based therapies (Juliano et al., 2020). The proposed neuro-marker supports the development of personalized "closed-loop" therapeutic VR environments where the choice and timing of virtual stimuli are synchronized with relevant, fluctuating brain states that modulate motor behavior, optimizing therapeutic efficacy (McDermott et al., 2023; Vourvopoulos et al., 2024). This allows for applications beyond traditional mirror therapy, such as visually experiencing the illusion of successful movements directly triggered by imagination and intention (McDermott et al., 2023). Additionally, "pre-assessments" of embodiment potential, utilizing this neuro-marker, could be used to predict and personalize EEG-based BCI therapy (Juliano et al., 2020).

Moreover, this research can effectively inform VR content and avatar design (Crone & Kallen, 2024; Genay et al., 2022; Kober et al., 2022). The degree of embodiment significantly influences user perception and behavior, including phenomena like the "Proteus Effect", where embodying a virtual avatar can alter a user's attitudes and behaviors (Genay et al., 2022; Juliano et al., 2020; Shin et al., 2021). Real-time SoA feedback can provide designers with critical data on which avatar representations or interaction methods are most effective in inducing or maintaining agency (Juliano et al., 2020; Shin et al., 2021). This is particularly relevant for tasks involving risk perception; while human-like avatars can enhance body ownership, they may also increase perceived risk and potentially degrade performance in high-risk teleoperation tasks (Shin et al., 2021). A real-time SoA measure could provide crucial data for designing avatars and interactions appropriate for specific task contexts (González-Franco et al., 2014; Shin et al., 2021). In the context of BCI tasks, it has been shown that using anthropomorphic avatars can increase the user's perceived agency and reduce frustration (Crone & Kallen, 2024; Ziadeh et al., 2021). The neuro-marker presented here provides an objective tool to robustly validate and explore this relationship.

Finally, this work contributes to advancing BCI technology, which allows users to control computers with their brain activity (Esteves et al., 2025; Jin et al., 2024; Nguyen et al., 2024). BCI systems often suffer from low performance and user frustration (Jin et al., 2024; Ziadeh et al., 2021). An objective SoA marker could help improve these systems by ensuring users feel in control (Cioffi et al., 2024; Juliano et al., 2020). Furthermore, the RP signal appears before a movement is executed. This predictive quality can be leveraged to create highly responsive "zero-lag" interfaces that anticipate a user's actions, which would dramatically improve the SoA (Brouwer et al., 2017; McDermott et al., 2023; Nguyen et al., 2024). By directly detecting the intention to move from the brain, this technology could also reduce the need for external tracking hardware, leading to more seamless and adaptive VR experiences (Dewil et al., 2023; Kritikos et al., 2023; Nwagu et al., 2023).

5. Limitations

Before mentioning methodological and technical limitations, it is worth noting that our discussion and interpretation of the results are based on indirect assumptions and analyses rather than direct demonstrations. As mentioned below, future studies could further investigate these hypotheses using more "direct" techniques and analyses such as fMRI or TMS. Taking this consideration into account, other limitations must be acknowledged. First, since this was the first study conducted on evoked potentials and VR environments with a focus on time delays, the specific delays selected for the study, i.e. 200, 400 and 600 ms, should be further decomposed (at least between the middle latencies, 200 and 400, where the sense of embodiment could be more challenged) to achieve more information on RP and its relationship with the avatar movement. Secondly, while EEG offers a unique window to observe the neural correlates of the relationship between real and virtual environments (Guy et al., 2023), it also poses various difficulties as the presence of movement artifacts in the recordings and the lack of spatial resolution (even though the presence of specific software as sLORETA offers a good compromise for evoked responses, it still does not offset the core problem of the technique). A way to overcome these difficulties could be to use other affordable and portable technologies such as functional near-infrared spectroscopy (fNIRS), less sensitive to movement and better able to detect specific cortical activations. Thirdly, we did not include trial-level kinematic covariates; future work should incorporate movement time/speed to further isolate pre-movement from execution-related neural variance, although our primary RP metrics were confined to the pre-movement interval. Finally, we did not directly measure the end-to-end latency of the VR tracking and rendering pipeline. Thus, future work should include explicit latency measurement and reporting.

6. Conclusions

In conclusion, this study provides compelling evidence that temporal discrepancies in avatar visuomotor synchrony systematically alter the Readiness Potential, in parallel with changes in subjective embodiment. We observed a shift in RP characteristics from central motor regions towards frontal activity, suggesting an increased engagement of higher-order cognitive processes like error monitoring in response to latency. These findings significantly advance our understanding of neural adaptation to virtual environments. Furthermore, these neurophysiological observations offer valuable insights for HCI, highlighting the RP as a potentially sensitive neuro-marker connected to embodiment and agency in VR. This connection suggests tangible pathways for enhancing interactive systems: it points towards tools for the real-time assessment that could inform personalized neurorehabilitation; offers potential for data-driven insights when optimizing avatar design and user engagement; and may support the development of predictive BCIs aimed at improving user control. By robustly linking specific EEG markers to user experience in VR, this research offers a foundational step towards creating more intuitive, responsive, and ultimately more effective immersive technologies.

CRediT authorship contribution statement

Alessandro Piedimonte: Writing – review & editing, Writing – original draft, Supervision, Resources, Methodology, Formal analysis, Data curation, Conceptualization. **Valeria Volpino:** Writing – review & editing, Writing – original draft, Investigation, Formal analysis. **Andrea Bottino:** Writing – review & editing, Supervision, Software, Resources, Methodology, Data curation, Conceptualization. **Francesco Strada:** Writing – review & editing, Software, Methodology, Conceptualization. **Fabio Cielo:** Software, Investigation. **Francesco Campaci:** Investigation. **Giorgia Cecconato:** Investigation. **Elisa Carlino:** Writing – review & editing, Writing – original draft, Supervision, Resources, Methodology, Data curation, Conceptualization.

Funding

Alessandro Piedimonte reports financial support was provided by Carlo Molo Onlus Foundation.

Declaration of competing interest

The authors declare that they have no known competing financial interests or personal relationships that could have appeared to influence the work reported in this paper.

Acknowledgments

We express our heartfelt gratitude to all those who participated in our study.

Appendix A. Embodiment questionnaire

See Tables A.1 and A.2.

Appendix B. sLORETA output

See Tables B.3–B.6.

Table A.1
Adapted embodiment questionnaire administered after each block.

ID	Question
Q1	"I felt out of my body"
Q2	"I felt as if the movements of the virtual body were influencing my own movements"
Q3	"I felt as if the virtual body was my body"
Q4	"I felt like I could control the virtual body as if it was my own body"

Table A.2
Means of embodiment questionnaire single items for all delay conditions.

Questions	NA-delay	200 ms	400 ms	600 ms
Q1	2.50	2.80	3.36	3.96
Q2	3.26	3.22	3.32	3.48
Q3	4.88	4.42	3.34	2.50
Q4	5.38	5.04	3.82	2.84

Table B.3
sLORETA output of the statistical comparison between the NA-delay > 200 ms conditions.

Brain region	Locations			Coordinates						*t*-values		N* v
	BA	Lobe	H	MNI			TAL			max	min	
Anterior cingulate	24, **32**, 33	Limbic	L/R	10	35	25	10	35	21	4.68	3.64	39
Medial frontal gyrus	**9**	Frontal	L/R	10	40	25	10	40	21	4.57	4.00	25
Cingulate gyrus	24, **32**	Limbic	L/R	5	35	30	5	35	26	4.32	3.60	17
Postcentral gyrus	**2**, 3	Parietal	R	45	−30	35	45	−27	34	4.14	3.59	13
Superior frontal gyrus	9, **10**	Frontal	R	25	45	30	25	45	25	4.03	3.58	8
Insula	**13**	Sub-lobar	R	35	−20	20	35	−18	19	3.93	3.58	14
Middle frontal gyrus	**10**	Frontal	R	30	45	30	30	45	25	3.92	3.66	2
Inferior parietal lobule	40	Parietal	R	45	−30	30	45	−28	29	3.91	3.67	5
Precentral gyrus	**4**	Frontal	R	45	−20	40	45	−18	38	3.80	3.64	2

Note. Bold numbers in the Brodmann Areas (BA) column stand for the area where the peak activity occurred; Montreal Neurological Institute (MNI) and Talairach (TAL) coordinates and t-values correspond to the most active voxel clusters in each brain region. N* v represents the number of active voxels.

Table B.4
sLORETA output of the statistical comparison between the NA-delay > 400 ms conditions.

Brain region	Locations			Coordinates						*t*-values		N* v
	BA	Lobe	H	MNI			TAL			max	min	
Cingulate gyrus	**32**, 24, 6, 23	Limbic	L/R	5	20	30	5	21	27	6.13	3.58	69
Anterior cingulate	**32**, 24, 33	Limbic	L/R	0	20	25	0	21	22	6.15	3.64	46
Medial frontal gyrus	**9**, 6	Frontal	L/R	5	30	35	5	31	31	5.51	3.61	38
Insula	13	Sub-lobar	L	−35	−15	15	−35	−14	15	4.15	3.62	19
Superior frontal gyrus	9	Frontal	R	10	50	30	10	50	25	4.44	3.61	11
Postcentral gyrus	**2**, 3	Parietal	R	40	−30	30	40	−28	29	3.76	3.56	8
Precentral gyrus	**6**, 4	Frontal	R	40	−10	35	40	−8	33	3.56	3.56	3
Inferior parietal lobule	40	Parietal	R	45	−30	30	45	−28	29	3.73	3.71	2

Note. Bold numbers in the Brodmann Areas (BA) column stand for the area where the peak activity occurred; Montreal Neurological Institute (MNI) and Talairach (TAL) coordinates and t-values correspond to the most active voxel clusters in each brain region. N* v represents the number of active voxels.

Table B.5
sLORETA output of the statistical comparison between the NA-delay > 600 ms conditions.

Brain region	Locations			Coordinates						*t*-values		N* v
	BA	Lobe	H	MNI			TAL			max	min	
Cingulate gyrus	**32**, 24, 6	Limbic, Frontal	L/R	−5	25	35	−5	26	31	5.04	3.64	29
Medial frontal gyrus	**9**, 6, 8	Frontal	L/R	−5	30	35	−5	31	31	4.99	3.62	31
Anterior cingulate	**24**, 32, 33	Limbic	L/R	−5	25	30	−5	26	26	5.00	3.59	24
Superior frontal gyrus	**8**, 6	Frontal	L/R	10	45	45	10	46	39	3.78	3.68	2
Precentral gyrus	6	Frontal	L	−25	−15	70	−25	−11	65	3.67	–	1
Middle frontal gyrus	6	Frontal	L	−25	−15	65	−25	−12	60	3.59	–	1

Note. Bold numbers in the Brodmann Areas (BA) column stand for the area where the peak activity occurred; Montreal Neurological Institute (MNI) and Talairach (TAL) coordinates and t-values correspond to the most active voxel clusters in each brain region. N* v represents the number of active voxels.

Table B.6
sLORETA output of the statistical comparison between the VR group > Real group.

Brain region	Locations			Coordinates						*t*-values		N* v
	BA	Lobe	H	MNI			TAL			max	min	
Superior frontal gyrus	**9**, 10	Frontal	L	−20	55	35	−20	55	29	3.76	3.42	33
Middle frontal gyrus	9, **10**	Frontal	L	−30	45	30	−30	45	25	3.71	3.39	10
Medial frontal gyrus	**10**	Frontal	L	−10	65	15	−10	64	11	3.45	3.38	4

Note. Bold numbers in the Brodmann Areas (BA) column stand for the area where the peak activity occurred; Montreal Neurological Institute (MNI) and Talairach (TAL) coordinates and t-values correspond to the most active voxel clusters in each brain region. N* v represents the number of active voxels.

Data availability

Data will be made available on request.

References

Abdlkarim, D., Di Luca, M., Aves, P., Maaroufi, M., Yeo, S.-H., Miall, R. C., Holland, P., & Galea, J. M. (2024). A methodological framework to assess the accuracy of virtual reality hand-tracking systems: A case study with the Meta Quest 2. *Behavior Research Methods*, *56*(2), 1052–1063. http://dx.doi.org/10.3758/s13428-022-02051-8.

Alchalabi, B., Faubert, J., & Labbe, D. (2019). EEG can be used to measure embodiment when controlling a walking Self-Avatar. In *2019 IEEE conference on virtual reality and 3D user interfaces (VR* (pp. 776–783). http://dx.doi.org/10.1109/VR.2019.8798263.

Argelaguet, F., Hoyet, L., Trico, M., & Lécuyer, A. (2016). The role of interaction in virtual embodiment: Effects of the virtual hand representation. *Proceedings - IEEE Virtual Reality*, http://dx.doi.org/10.1109/VR.2016.7504682.

Bedir, D., & Erhan, S. (2021). The effect of virtual reality technology on the imagery skills and performance of Target-Based sports Athletes. *Frontiers in Psychology*, *11*, http://dx.doi.org/10.3389/fpsyg.2020.02073.

Bockelmann, N., Fischer, R., & Zachmann, G. (2024). Embodiment in virtual Environments-Analyzing the effects of latency and avatar representation. In *2024 international conference on cyberworlds* (pp. 17–24). IEEE, http://dx.doi.org/10.1109/CW64301.2024.00012.

Botvinick, M., & Cohen, J. (1998). Rubber hands "feel" touch that eyes see [8]. *Nature*, *391*(ue 6669), http://dx.doi.org/10.1038/35784.

Braun, N., Debener, S., Spychala, N., Bongartz, E., Sörös, P., Müller, H., & Philipsen, A. (2018). The senses of agency and ownership: A review. *Frontiers in Psychology*, *9*(ue APR), http://dx.doi.org/10.3389/fpsyg.2018.00535.

Brouwer, A.-M., Waa, J., Hogervorst, M., Cacace, A., & Stokking, H. (2017). A feasible BCI in real life: Using predicted head rotation to improve HMD imaging. In *Proceedings of the 2017 ACM workshop on an application-oriented approach to BCI out of the laboratory* (pp. 35–38). http://dx.doi.org/10.1145/3038439.3038440.

Burns, C., & Fairclough, S. (2015). Use of auditory event-related potentials to measure immersion during a computer game. *International Journal of Human-Computer Studies*, *73*, 107–114. http://dx.doi.org/10.1016/j.ijhcs.2014.09.002.

Carlino, E., Piedimonte, A., Romagnolo, A., Guerra, G., Frisaldi, E., Vighetti, S., Lopiano, L., & Benedetti, F. (2019). Verbal communication about drug dosage balances drug reduction in Parkinson's disease: behavioral and electrophysiological evidences. *Parkinsonism & Related Disorders*, *65*, 184–189. http://dx.doi.org/10.1016/j.parkreldis.2019.06.015.

Caserman, P., Martinussen, M., & Göbel, S. (2019). Effects of end-to-end latency on user experience and performance in immersive virtual reality applications. In *Joint international conference on entertainment computing and serious games* (pp. 57–69). Springer, http://dx.doi.org/10.1007/978-3-030-34644-7_5.

Cioffi, E., Hutber, A., Molloy, R., Murden, S., Yurkewich, A., Kirton, A., Lin, J.-P., Gimeno, H., & McClelland, V. (2024). EEG-based sensorimotor neurofeedback for motor neurorehabilitation in children and adults: A scoping review. *Clinical Neurophysiology*, *167*, 143–166. http://dx.doi.org/10.1016/j.clinph.2024.08.009.

Crone, C., & Kallen, R. (2024). Measuring virtual embodiment: A psychometric investigation of a standardised questionnaire for the psychological sciences. *Computers in Human Behavior Reports*, *14*, Article 100422. http://dx.doi.org/10.1016/j.chbr.2024.100422.

Delorme, A., & Makeig, S. (2004). EEGLAB: An open source toolbox for analysis of single-trial EEG dynamics including independent component analysis. *Journal of Neuroscience Methods*, *134*(1), http://dx.doi.org/10.1016/j.jneumeth.2003.10.009.

Dewil, S., Kuptchik, S., Liu, M., Sanford, S., Bradbury, T., Davis, E., Clemente, A., & Nataraj, R. (2023). The cognitive basis for virtual reality rehabilitation of upper-extremity motor function after neurotraumas. *Journal on Multimodal User Interfaces*, *17*(3), 105–120. http://dx.doi.org/10.1007/s12193-023-00406-9.

Ehrsson, H., Spence, C., & Passingham, R. (2004). That's my hand! Activity in premotor cortex reflects feeling of ownership of a limb. *Science*, *305*(5685), http://dx.doi.org/10.1126/science.1097011.

Esteves, D., Valente, M., Bendor, S., Andrade, A., & Vourvopoulos, A. (2025). Identifying EEG biomarkers of sense of embodiment in virtual reality: Insights from spatio-spectral features. *Frontiers in Neuroergonomics*, *6*, http://dx.doi.org/10.3389/fnrgo.2025.1572851.

Faul, F., Erdfelder, E., Lang, A., & Buchner, A. (2007). G*Power 3: A flexible statistical power analysis program for the social, behavioral, and biomedical sciences. *Behavior Research Methods*, *39*(2), http://dx.doi.org/10.3758/BF03193146.

Feder, S., Miksch, J., Grimm, S., Krems, J., & Bendixen, A. (2023). Using event-related brain potentials to evaluate motor-auditory latencies in virtual reality. *Frontiers in Neuroergonomics*, *4*, http://dx.doi.org/10.3389/fnrgo.2023.1196507.

Garbarini, F., Fornia, L., Fossataro, C., Pia, L., Gindri, P., & Berti, A. (2014). Embodiment of others' hands elicits arousal responses similar to one's own hands. *Current Biology*, *24*(ue 16), http://dx.doi.org/10.1016/j.cub.2014.07.023.

Garbarini, F., Pia, L., Piedimonte, A., Rabuffetti, M., Gindri, P., & Berti, A. (2013). Embodiment of an alien hand interferes with intact-hand movements. *Current Biology*, *23*(ue 2), http://dx.doi.org/10.1016/j.cub.2012.12.003.

Genay, A., Lécuyer, A., & Hachet, M. (2022). Being an Avatar "for Real": A survey on virtual embodiment in augmented reality. *IEEE Transactions on Visualization and Computer Graphics*, *28*(12), 5071–5090. http://dx.doi.org/10.1109/TVCG.2021.3099290.

Gerardin, E., Sirigu, A., Lehericy, S., Poline, J., Gaymard, B., Marsault, C., Agid, Y., & Le Bihan, D. (2000). Partially overlapping neural networks for real and imagined hand movements. *Cerebral Cortex*, *10*(11), http://dx.doi.org/10.1093/cercor/10.11.1093.

González-Franco, M., Peck, T., Rodríguez-Fornells, A., & Slater, M. (2014). A threat to a virtual hand elicits motor cortex activation. *Experimental Brain Research*, *232*(3), 875–887. http://dx.doi.org/10.1007/s00221-013-3800-1.

Grivaz, P., Blanke, O., & Serino, A. (2017). Common and distinct brain regions processing multisensory bodily signals for peripersonal space and body ownership. *NeuroImage*, *147*, http://dx.doi.org/10.1016/j.neuroimage.2016.12.052.

Guy, M., Normand, J.-M., Jeunet-Kelway, C., & Moreau, G. (2023). The sense of embodiment in Virtual Reality and its assessment methods. In *Frontiers in virtual reality*. *Frontiers in Virtual Reality*, *vol. 4*, http://dx.doi.org/10.3389/frvir.2023.1141683.

Haaland, K., Harrington, D., & Knight, R. (2000). Neural representations of skilled movement. *Brain*, *123*(11), http://dx.doi.org/10.1093/brain/123.11.2306.

Hanakawa, T., Immisch, I., Toma, K., Dimyan, M., Gelderen, P., & Hallett, M. (2003). Functional properties of brain areas associated with motor execution and imagery. *Journal of Neurophysiology*, *89*(2), http://dx.doi.org/10.1152/jn.00132.2002.

Im, H., Ku, J., Kim, H., & Kang, Y. (2016). Virtual reality-guided motor imagery increases corticomotor excitability in healthy volunteers and stroke patients. *Annals of Rehabilitation Medicine*, *40*(3), http://dx.doi.org/10.5535/arm.2016.40.3.420.

Jäncke, L., Cheetham, M., & Baumgartner, T. (2009). Virtual reality and the role of the prefrontal cortex in adults and children. *Frontiers in Neuroscience*, *3*(ue MAY), http://dx.doi.org/10.3389/neuro.01.006.2009.

Jeunet, C., Albert, L., Argelaguet, F., & Lécuyer, A. (2018). Do you feel in control?": Towards novel approaches to characterise, manipulate and measure the sense of agency in virtual environments. *IEEE Transactions on Visualization and Computer Graphics*, *24*(4), 1486–1495. http://dx.doi.org/10.1109/TVCG.2018.2794598.

Jin, W., Zhu, X., Qian, L., Wu, C., Yang, F., Zhan, D., Kang, Z., Luo, K., Meng, D., & Xu, G. (2024). Electroencephalogram-based adaptive closed-loop brain-computer interface in neurorehabilitation: A review. *Frontiers in Computational Neuroscience*, *18*, http://dx.doi.org/10.3389/fncom.2024.1431815.

Juliano, J., Spicer, R., Vourvopoulos, A., Lefebvre, S., Jann, K., Ard, T., Santarnecchi, E., Krum, D., & Liew, S.-L. (2020). Embodiment is related to better performance on a Brain–Computer interface in immersive virtual reality: A Pilot study. *Sensors*, *20*(4), http://dx.doi.org/10.3390/s20041204.

Jung, T., Makeig, S., Humphries, C., Lee, T., Mckeown, M., Iragui, V., & Sejnowski, T. (2000). Removing electroencephalographic artifacts by blind source separation. *Psychophysiology*, *37*(2), http://dx.doi.org/10.1017/S0048577200980259.

Kim, H., Wright, D., Rhee, J., & Kim, T. (2023). C3 in the 10-20 system may not be the best target for the motor hand area. *Brain Research*, http://dx.doi.org/10.1016/j.brainres.2023.148311.

Kober, S., Settgast, V., Brunnhofer, M., Augsdörfer, U., & Wood, G. (2022). Move your virtual body: Differences and similarities in brain activation patterns during hand movements in real world and virtual reality. *Virtual Reality*, *26*(2), 501–511. http://dx.doi.org/10.1007/s10055-021-00588-1.

Kornhuber, H., & Deecke, L. (1965). Hirnpotentialänderungen bei willkürbewegungen und passiven bewegungen des menschen: Bereitschaftspotential und reafferente potentiale. *Pflügers Archiv für die Gesamte Physiologie des Menschen und der Tiere*, *284*(1), http://dx.doi.org/10.1007/BF00412364.

Kritikos, J., Makrypidis, A., Alevizopoulos, A., Alevizopoulos, G., & Koutsouris, D. (2023). Can Brain–Computer interfaces replace virtual reality controllers? A machine learning movement prediction model during virtual reality simulation using EEG recordings. *Virtual Worlds*, *2*(2), http://dx.doi.org/10.3390/virtualworlds2020011.

Lui, K., Nunez, M., Cassidy, J., Vandekerckhove, J., Cramer, S., & Srinivasan, R. (2021). Timing of readiness potentials reflect a Decision-making process in the human brain. *Computational Brain and Behavior*, *4*(3), http://dx.doi.org/10.1007/s42113-020-00097-5.

Mazziotta, J., Toga, A., Evans, A., Fox, P., Lancaster, J., Zilles, K., Woods, R., Paus, T., Simpson, G., Pike, B., Holmes, C., Collins, L., Thompson, P., MacDonald, D., Iacoboni, M., Schormann, T., Amunts, K., Palomero-Gallagher, N., Geyer, S., & Mazoyer, B. (2001). A probabilistic atlas and reference system for the human brain: International consortium for brain mapping (ICBM. *Philosophical Transactions of the Royal Society, Series B (Biological Sciences)*, *356*(ue 1412), http://dx.doi.org/10.1098/rstb.2001.0915.

McDermott, E., Metsomaa, J., Belardinelli, P., Grosse-Wentrup, M., Ziemann, U., & Zrenner, C. (2023). Predicting motor behavior: An efficient EEG signal processing pipeline to detect brain states with potential therapeutic relevance for VR-based neurorehabilitation. *Virtual Reality*, *27*(1), 347–369. http://dx.doi.org/10.1007/s10055-021-00538-x.

Meehan, M., Insko, B., Whitton, M., & Brooks, F. (2002). Physiological measures of presence in stressful virtual environments. In *Proceedings of the 29th annual conference on computer graphics and interactive techniques, SIGGRAPH '02* (pp. 645–652). http://dx.doi.org/10.1145/566570.566630.

Menon, V., & D'Esposito, M. (2022). The role of PFC networks in cognitive control and executive function. *Neuropsychopharmacology*, *47*(ue 1), http://dx.doi.org/10.1038/s41386-021-01152-w.

Nguyen, W., Gramann, K., & Gehrke, L. (2024). Modeling the intent to interact with VR using physiological features. *IEEE Transactions on Visualization and Computer Graphics*, *30*(8), 5893–5900. http://dx.doi.org/10.1109/TVCG.2023.3308787.

Nichols, T., & Holmes, A. (2002). Nonparametric permutation tests for functional neuroimaging: A primer with examples. *Human Brain Mapping*, *15*(1), http://dx.doi.org/10.1002/hbm.1058.

Nwagu, C., AlSlaity, A., & Orji, R. (2023). EEG-Based Brain-Computer interactions in immersive virtual and augmented reality: A systematic review. *Proceedings of the ACM on Human-Computer Interaction*, *7*(EICS), http://dx.doi.org/10.1145/3593226.

Pascual-Marqui, R. (2002). Standardized low-resolution brain electromagnetic tomography (sLORETA): Technical details. *Methods and Findings in Experimental and Clinical Pharmacology*, *24*(SUPPL. D).

Peck, T., & Gonzalez-Franco, M. (2021). Avatar embodiment. A standardized questionnaire. *Frontiers in Virtual Reality*, *1*, http://dx.doi.org/10.3389/frvir.2020.575943.

Pia, L., Fossataro, C., Burin, D., Bruno, V., Spinazzola, L., Gindri, P., Fotopoulou, K., Berti, A., & Garbarini, F. (2020). The anatomo-clinical picture of the pathological embodiment over someone else's body part after stroke. *Cortex*, *130*, http://dx.doi.org/10.1016/j.cortex.2020.05.002.

Piedimonte, A., Benedetti, F., & Carlino, E. (2015). Placebo-induced decrease in fatigue: Evidence for a central action on the preparatory phase of movement. *European Journal of Neuroscience*, *41*(4), http://dx.doi.org/10.1111/ejn.12806.

Pion-Tonachini, L., Kreutz-Delgado, K., & Makeig, S. (2019). ICLabel: An automated electroencephalographic independent component classifier, dataset, and website. *NeuroImage*, *198*, http://dx.doi.org/10.1016/j.neuroimage.2019.05.026.

Porssut, T., Herbelln, B., & Boulic, R. (2019). Reconciling being in-control vs. being helped for the execution of complex movements in VR. In *26th IEEE conference on virtual reality and 3D user interfaces, VR 2019 - proceedings* (pp. 529–537). http://dx.doi.org/10.1109/VR.2019.8797716.

Raz, G., Gurevitch, G., Vaknin, T., Aazamy, A., Gefen, I., Grunstein, S., Azouri, G., & Goldway, N. (2020). Electroencephalographic evidence for the involvement of mirror-neuron and error-monitoring related processes in virtual body ownership. *NeuroImage*, *207*, http://dx.doi.org/10.1016/j.neuroimage.2019.116351.

Rigoni, D., Kühn, S., Sartori, G., & Brass, M. (2011). Inducing disbelief in free will alters brain correlates of preconscious motor preparation: The brain minds whether we believe in free will or not. *Psychological Science*, *22*(5), http://dx.doi.org/10.1177/0956797611405680.

Ruess, M., Thomaschke, R., & Kiesel, A. (2017). The time course of intentional binding. *Attention, Perception, & Psychophysics*, *79*(4), 1123–1131. http://dx.doi.org/10.3758/s13414-017-1292-y.

Safikhani, S., Gattringer, V., Schmied, M., Pirker, J., & Wriessnegger, S. (2024). The influence of realism on the sense of presence in virtual reality: Neurophysiological insights using EEG. *Multimodal Technologies and Interaction*, *8*(11), http://dx.doi.org/10.3390/mti8110104.

Samaraweera, G., Guo, R., & Quarles, J. (2013). Latency and avatars in virtual environments and the effects on gait for persons with mobility impairments. In *2013 IEEE symposium on 3D user interfaces (3DUI* (pp. 23–30). IEEE, http://dx.doi.org/10.1109/VR.2013.6549378.

Sasaoka, T., Hirose, K., Maekawa, T., Inui, T., & Yamawaki, S. (2024). The anterior cingulate cortex is involved in intero-exteroceptive integration for spatial image transformation of the self-body. *NeuroImage*, *293*, Article 120634. http://dx.doi.org/10.1016/j.neuroimage.2024.120634.

Schultze-Kraft, M., Parés-Pujolràs, E., Matić, K., Haggard, P., & Haynes, J.-D. (2020). Preparation and execution of voluntary action both contribute to awareness of intention. *Proceedings of the Royal Society B*, *287*(1923), Article 20192928. http://dx.doi.org/10.1098/rspb.2019.2928.

Schurger, A., Hu, P., Pak, J., & Roskies, A. (2021). What is the readiness potential? *Trends in Cognitive Sciences*, *25*(ue 7), http://dx.doi.org/10.1016/j.tics.2021.04.001.

Shibasaki, H., & Hallett, M. (2006). What is the bereitschaftspotential? *Clinical Neurophysiology*, *117*(ue 11), http://dx.doi.org/10.1016/j.clinph.2006.04.025.

Shibuya, S., Unenaka, S., Zama, T., Shimada, S., & Ohki, Y. (2019). Sensorimotor and posterior brain activations during the observation of illusory embodied fake hand movement. *Frontiers in Human Neuroscience*, *13*, http://dx.doi.org/10.3389/fnhum.2019.00367.

Shin, M., Lee, S., Song, S., & Chung, D. (2021). Enhancement of perceived body ownership in virtual reality-based teleoperation may backfire in the execution of high-risk tasks. *Computers in Human Behavior*, *115*, Article 106605. http://dx.doi.org/10.1016/j.chb.2020.106605.

Silva, L., Amitai, Y., & Connors, B. (1991). Intrinsic oscillations of neocortex generated by layer 5 pyramidal neurons. *Science*, *251*(4992), http://dx.doi.org/10.1126/science.1824881.

StatSoft, I. (2011). STATISTICA (data analysis software system), version 10.

Suviseshamuthu, E., Shenoy Handiru, V., Allexandre, D., Hoxha, A., Saleh, S., & Yue, G. (2022). EEG-Based spectral analysis showing brainwave changes related to modulating progressive fatigue during a prolonged intermittent motor task. *Frontiers in Human Neuroscience*, *16*, http://dx.doi.org/10.3389/fnhum.2022.770053.

Tan, G., Uchitomi, H., Isobe, R., & Miyake, Y. (2024). Sense of embodiment with synchronized avatar during walking in mixed reality. *Scientific Reports*, *14*(1), 21198. http://dx.doi.org/10.1038/s41598-024-72095-7.

Vourvopoulos, A., Fleury, M., Blanco-Mora, D. A., Fernandes, J.-C., Figueiredo, P., & i Badia, S. B. (2024). Brain imaging and clinical outcome of embodied VR-BCI training in chronic stroke patients: A longitudinal pilot study. *Brain-Computer Interfaces*, *11*(4), 193–209. http://dx.doi.org/10.1080/2326263X.2024.2409463.

Waltemate, T., Senna, I., Hülsmann, F., Rohde, M., Kopp, S., Ernst, M., & Botsch, M. (2016). The impact of latency on perceptual judgments and motor performance in closed-loop interaction in virtual reality. In *Proceedings of the 22nd ACM conference on virtual reality software and technology* (pp. 27–35). http://dx.doi.org/10.1145/2993369.2993381.

Wegner, D., & Wheatley, T. (1999). Apparent mental causation: Sources of the experience of will. *American Psychologist*, *54*(7), http://dx.doi.org/10.1037/0003-066X.54.7.480.

Wen, W., Minohara, R., Hamasaki, S., Maeda, T., An, Q., Tamura, Y., Yamakawa, H., Yamashita, A., & Asama, H. (2018). The readiness potential reflects the reliability of action consequence. *Scientific Reports*, *8*(1), http://dx.doi.org/10.1038/s41598-018-30410-z.

Ziadeh, H., Gulyas, D., Nielsen, L., Lehmann, S., Nielsen, T., Kjeldsen, T., Hougaard, B., Jochumsen, M., & Knoche, H. (2021). Mine works better": Examining the influence of embodiment in virtual reality on the sense of agency during a binary motor imagery task with a Brain-Computer interface. *Frontiers in Psychology*, *12*, http://dx.doi.org/10.3389/fpsyg.2021.806424.

Zilles, K., & Amunts, K. (2010). Centenary of Brodmann's map conception and fate. *Nature Reviews. Neuroscience*, *11*(ue 2), http://dx.doi.org/10.1038/nrn2776.